Monterey Bay Aquarium
Research Institute

Machine learning facilitates the study of gelatinous zooplankton, *Benthocodon pedunculata*, abundance over six years in the Northeast Pacific abyssal plain.

Giovanna Sainz, University of California, Santa Cruz

Krish Mehta, California Institute of Technology

Mentors: Dr. Kakani Katija, Dr. Christine Huffard and Dr. Eric Orenstein

Summer 2021

Keywords: Benthic Boundary Layer, Hydromedusae, Station M, Machine Learning

1. ABSTRACT

Understanding the ecological variability of deep-sea organisms is critical for the preservation and protection of deep-sea ecosystems. Many animals, including gelatinous zooplankton, are commonly found within the benthic boundary layer (BBL), an important region in the water column that is essential for pelagic-benthic coupling processes (e.g. carbon and nutrient cycling). BBL processes, and changes in animal communities, have been studied at Station M (~ 4,000 m deep in Northeast Pacific) since 1989. In this present study we ask: how does animal abundance change in the BBL in relation to time? With its distinct identification features and observed high densities at Station M, the gelatinous hydrozoan, Benthocodon pedunculata, makes an ideal study candidate. Specifically, we looked for seasonality in the abundance of these hydromedusae and whether some years experienced higher densities. To achieve this, we leveraged 30 years of visual data collection at Station M, which includes remotely operated vehicle (ROV) video transects, still images from time-lapse cameras and a seafloor-transiting benthic rover. To analyze this high volume of imagery, we applied machine learning (ML) by (1) training

a multi-object benthic classifier on MBARI's VARS data; (2) deployed the classifier on the image data to generate proposals for classifications and localizations; and (3) reviewed the ML proposals of B. pedunculata using the vars-gridview tool. Preliminary results indicate that there is variation in their abundance.

2. INTRODUCTION

The Benthic boundary layer (BBL) is an enriched water column directly above the seafloor. It's associated with critical biogeochemical processes between the pelagic and benthic regions of the deep-sea (Smith, 1992). This includes the transport of organic particles to the seafloor, contributing to carbon cycling in the ocean (Boudreau & Jorgensen, 2001; Thomsen, 1999). In addition, this water column has observed high abundances of gelatinous marine organisms including deep-sea jellies (Wishner, 1980) therefore, it's been suggested that most of the species in the BBL play an important role in the pelagic-benthic marine food web (Alldredge, 1984; Choy et al., 2017; Gibson & Barnes, 1997).

The gelatinous hydrozoan, *Benthocodon pedunculata* (Order: Trachymedusae, Family: Rhopalonematidae), has often been observed at high densities in the BBL within Station M (4000 m depth), a time-series station collecting data for over 30 years. These small medusae reach up to 3 cm in diameter and can be characterized by their deep reddish-brown coloration, rounded bell, and their numerous short tentacles (up to ~350) (Fig.1). They are commonly found in the Monterey submarine canyon (deeper than 3000m) but have also been observed in the Atlantic and other regions of the Pacific Ocean (Larson et al., 1992; Matsumoto et al., 1997, 2020).

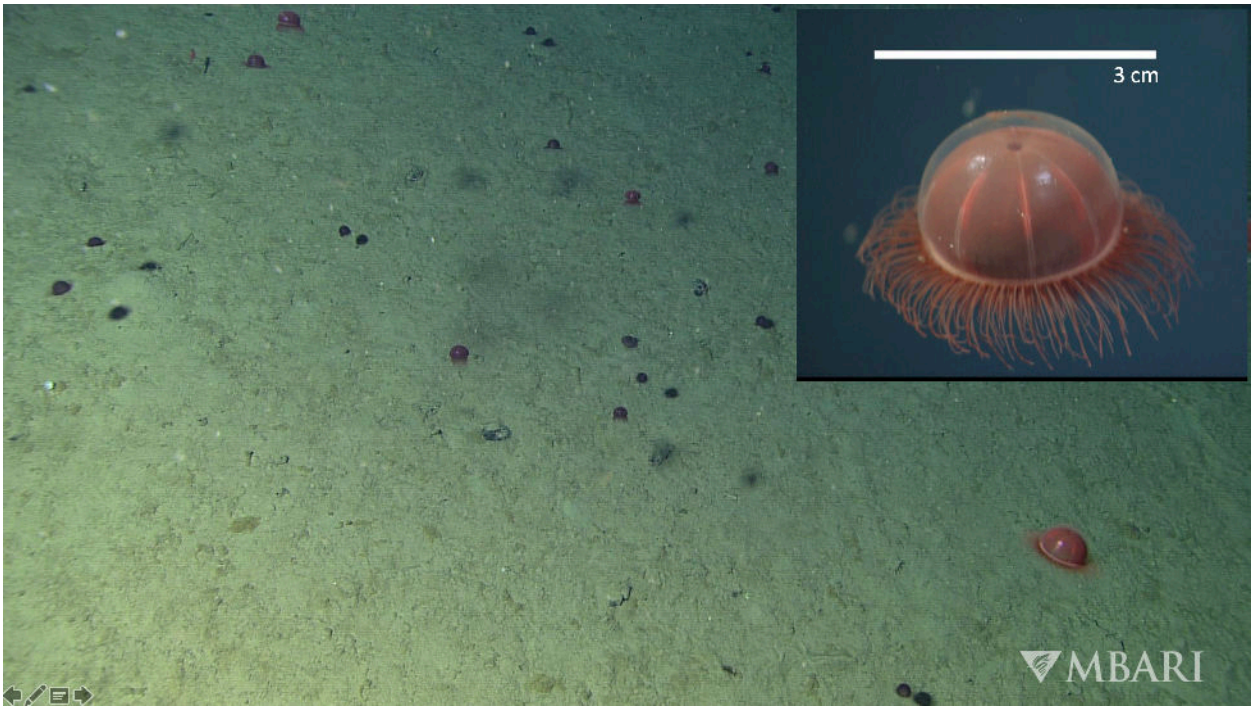

Figure 1. (Top right) Close-up of species of interest *Benthocodon pedunculata. (Background)*A dense swarm of *B. pedunculata* in the Monterey abyssal plain. Image credits: Monterey Bay Research Institute.

B. pedunculata is typically observed above (up to 100 m) or directly on the seafloor. Specifically, regions of the seafloor that are covered by soft sediment. These observations of them resting on the seafloor have suggested that they feed off the bottom (Matsumoto et al., 1997). A large portion of their diet consists of foraminiferans and crustaceans like copepods and amphipods which are mostly benthic (Gage & Tyler, 1991).

Although it's a common inhabitant within the BBL at Station M, the ecological role of this benthopelagic medusae is poorly understood. In order to get an understanding of their importance in the food web, there is a need to investigate how their populations vary over time. In this present study, we investigated the abundance patterns of the hydromedusae *Benthocodon pedunculata* in the Benthic Boundary layer at Station M, using machine learning as a tool. Methods of obtaining *B. pedunculata* density were used from a 3-year time-series study by (Smith et al., 2020). We wanted to know whether some years experienced higher densities over a 6-year period between the years 2013-2019.

3. MATERIALS AND METHODS

3.1 Area of study

Station M (34°50′N, 123°00′W, 4000m) is located in the Monterey abyssal plain of the Northeast Pacific and is about 291 kilometers offshore of Santa Barbara, CA (Fig. 2). This area is characterized by soft sediment (silty-clay) and low topographic relief (<100 m over 1600 km2) (Smith & Druffel, 1998). Station M has been collecting visual data of the seafloor for the past 30 years. It hosts a variety of imaging systems and is one of three long-term monitoring study sites of the abyssal plain in the world ("Station M Instrument Servicing Expedition 2018," 2018). Instrumentation includes the benthic rover, an autonomous robot that moves slowly across the seafloor collecting photos and sediment measurements, sediment traps that collect sinking organic particles that sink down to the seafloor, time-lapse cameras, and yearly visits from MBARI's remotely operated vehicles.

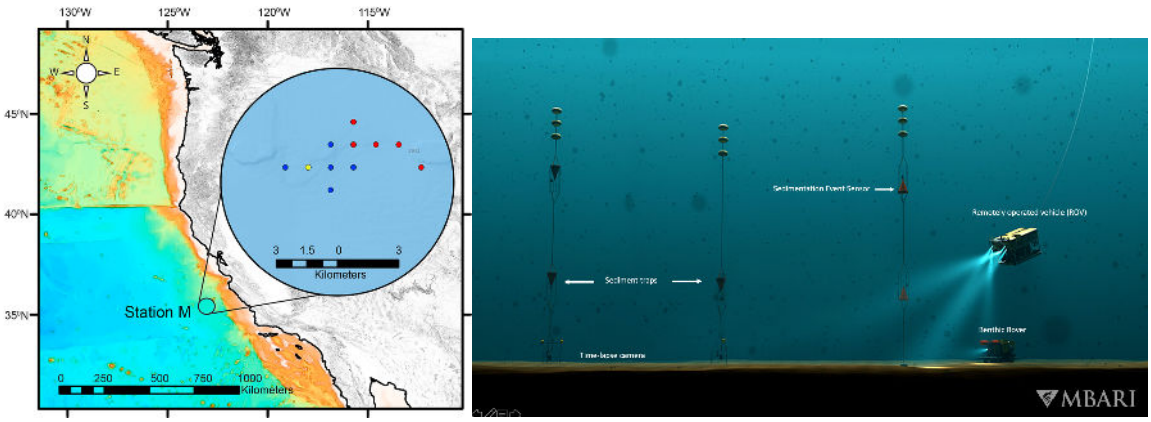

Figure 2. (Left) Map of Station M. The enlarged area presents the location of imaging instruments at Sta M, such as the time-lapse camera (yellow) and the benthic rover (blue). The red dots represent ROV dive sites. Figure credit: (Smith et al., 2020). (Right) Graphic depicts instrumentation from Station M ("Station M Instrument Servicing Expedition 2018," 2018).

For this study, we focused on imagery from a time-lapse camera (CANON 5D Mark iii) supported by a titanium tripod where the lens of the camera was resting 2.05m above the seabed. On each side of the tripod was a 200W strobe that provided illumination to the seafloor. The camera was tilted down 32° degrees which gave a field of view volume of 13.7m³ (Smith et al., 2020). Lighting quality in the top 20% of each image was not favorable making it difficult to identify marine organisms, therefore, only the bottom 80% of each image was analyzed, yielding

a sample volume of 19.3 m^3 (Fig. 3). Photographs were taken every hour, although there are some periods of 2013 that were not recorded.

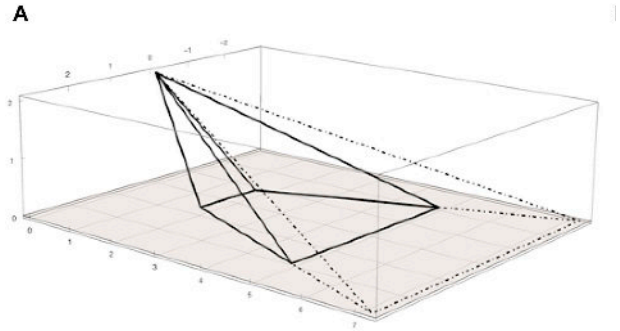

Figure 3. Solid black line represents the sample volume (19.3 m^3) of analyzing 80% of the image. Figure credit: (Smith et.al., 2020).

3.2 Machine learning applications (ML)- Model

A YOLOV5 deep learning model for object detection (Redmon et al., 2016) was applied in this study. This is a form of supervised machine learning and it generates a bounding box around individual objects of interest within each image, a class label, and a confidence score (Fig. 4). The model was run on 47,114 images from Station M's time-lapse camera between June 2013-December 2019 with a confidence threshold of 0.1, where the detections of B. pedunculata were recorded.

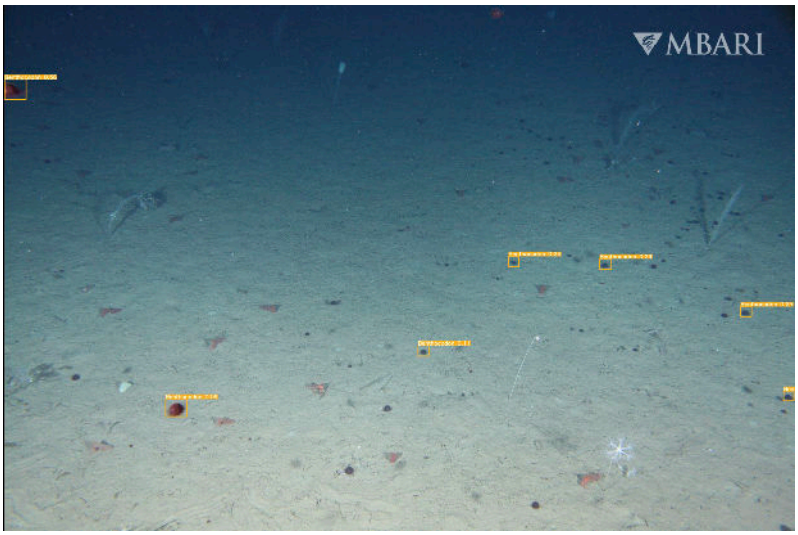

Figure 4. Image from VARS database that shows a swarm of *B.pedunculata* in the Monterey abyssal plain. The orange bounding boxes were generated by the YOLOV5 model and include class label and confidence score.

3.3 ML Image training & testing sets

To generate training data for the application of machine learning, images from ROV dives containing *Benthocodon* were queried within VARS-Localizer, a software tool that queries observational annotations from MBARI's Video Annotation and Reference System (VARS). VARS is an open-source database that stores and catalogs deep-sea imagery collected by MBARI's different camera systems including dives by remotely operated vehicles (Schlining & Stout, 2006). Within each image, bounding boxes or "localizations" were manually created around each individual (Fig.4). Over 1000 localizations of *Benthocodon* were labeled in Genus (*Benthocodon*, 662) and species level (*B. pedunculata,* 572) combined. To quickly correct and edit bounding boxes, VARS-gridview (Fig.5), an MBARI-developed software was utilized (Vars-Gridview, 2021/2021).

Testing data was generated using RectLabel software (RectLabel- Lableing Images for Bounding Box Object Detection and Segmentation, n.d). A subset of 235 randomly selected unlabeled images from Station M's time-lapse camera were manually labeled. This testing data was used to evaluate model performance.

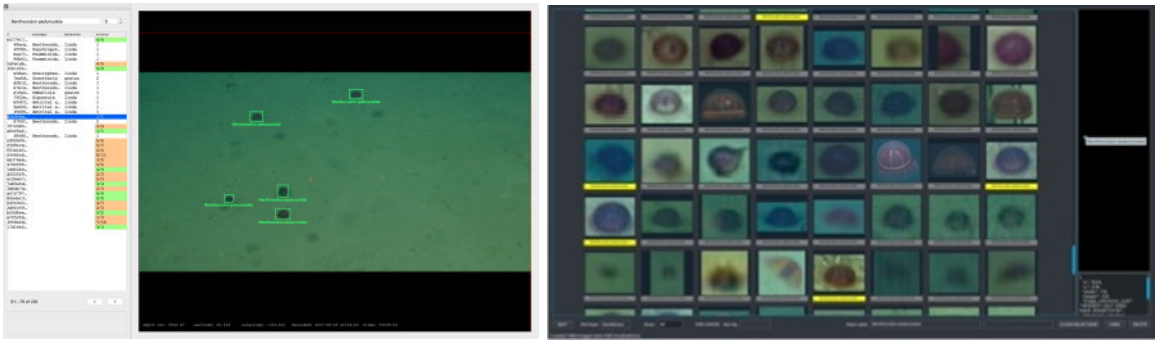

Figure 5. (Left) VARS-Localizer enables the labeling of visual data directly from the VARS database. Green boxes are the localizations generated by an person annotator. (Right) VARS-gridview displays each individual *Benthocodon* localization making it easier to correct or resize bounding boxes.

3.4 Verification and analysis of ML Performance

Once the ML classifier was applied to unlabeled Station M images, we evaluated the performance of the model by randomly selecting a subset of 250 images representing the years of interest (2013-2019). For each image, we recorded: (1) True positives (TP): Number of correctly identified objects, (2) False positives (FP): Number of incorrectly identified objects (e.g. calling a sea cucumber *Benthocodon*) (3) False negatives (FN): Number of target objects missed by the

model. This information allowed us to calculate the error estimate of *Benthocodon* counts generated by the model to give a more accurate number, under the assumption that the model cannot be 100 percent accurate. To find the total true objects, we used the following equations:

$$(1)\ Precision = \frac{TP}{TP + FN}$$

$$(2)\ Recall = \frac{TP}{TP + FP}$$

In Eq. 1, the precision gives the proportion between the number of positives the model detects and all of the objects in the image. This is a measure of the accuracy of the predictions generated by the model. Eq. 2, is the proportion of correct detections by the model and the actual count of the object of interest. This indicates how good the model is at correctly classifying the object of interest. Once precision and recall were calculated, the error estimated total object count was found by using the following equation:

$$(3)\ Total\ number\ of\ Benthocodon = \frac{(recall * detections)}{precision}$$

3.5 Calculating density of Benthocodon

To calculate the density and plot our time-series graph of *Benthocodon*, we used R 4.1.0 (R Core Team, 2013) and R Studio 1.4.1717. To find density we used:

$$(4)\ Density = \frac{\#\ of\ Benthocodon}{Sample\ volume}, (units = {Individuals}/{\mathrm{m}^3})$$

For Eq.4, monthly densities were calculated from 2013-2019.

4. RESULTS

4.1 Analysis of ML performance

An average of 11.4% of *Benthocodon* were detected by the YOLOV5 model. In images that had high densities (60+) of *Benthocodon* in frame, the model detected an average of 7-8 target objects. Our model precision was 81.6%.

4.2 Benthocodon density over time

Variation in the abundance of *Benthocodon* over a 6-year time period was observed in our preliminary results. The highest density recorded were in the years 2015 and 2016 with a density average of over 0.6 individuals·m^{-3}. Low densities were observed in 2016 and 2018 with a density average of ~0.05·m^{-3} (Fig. 6).

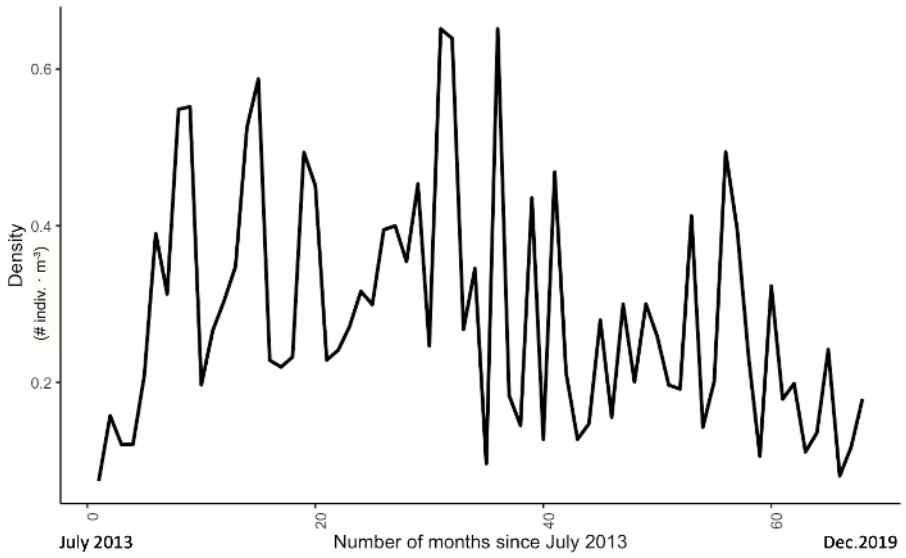

Figure 6. Time-series graph shows the monthly density *of Benthocodon pedunculata (*y-axis) through time (x-axis) from July 2013-Decemeber 2019. The counts of *Benthocodon* were generated from the machine learning proposals.

DISCUSSION

Although we were able to plot a time-series graph with the output generated by our machine learning model, we cannot make concrete conclusions about the variability observed in this time-series study. Our model detected a low percentage (11.4%) of *Benthocodon* when deployed on unlabeled images from Station M. The more objects in the image, the less accurate the model seemed to be. In addition, training a model on a small object like *Benthocodon* proved to be a challenging task. *Benthocodon* appears indistinct the smaller and further away it is in the image. Our model did not detect these smaller target species. It's also important to note that most of the training data generated came from ROV dives. The camera field of view varies across dives. Most of the images within VARS have close-up views of our target species, with few representing a similar field of view as the time-lapse camera images from station M. Lighting can also vary between the ROV dives and the time-lapse camera at Station M which may have contributed to the low accuracy of the model. A suggestion for future work would be to generate a Station M-specific training set. This may yield higher detection and classification of our target species.

Despite the low detection rate of our target species, our study was still able to yield population counts and would greatly benefit from ML model improvements. Our preliminary results suggest investing in creating more image training sets can increase the capability to accurately detect and classify marine organisms. Machine learning has the potential to further advance our understanding of our oceans and answer ecological questions. Once a more accurate representation of abundance over time is achieved, future studies could see if environmental factors play a role in abundance changes over time. Things like current speed, food availability, and substrate type. In situ studies have suggested that substrate type and current speed may have an effect on the abundance of *Benthocodon* (Matsumoto et al., 1997). Results from a 3-year time-series study at Sta. M found that ocean currents seem to influence the abundance of *B .pedunculata*. As current speed increased, the density of *Benthocodon* decreased suggesting that they swim high above the seafloor when current speed is high (Smith et al., 2020). Having this knowledge of abundance can provide some insight on deep-sea jelly community structure in the BBL and its

significance in the benthopelagic food web, which can lead to the overall important goal of protecting and preserving these deep-sea ecosystems.

ACKNOWLEDGEMENTS

First, I would like to thank my mentors Dr. Kakani Katija, Dr. Christine Huffard, and Dr. Orenstein for all of their support and encouragement during this internship. Everything from sharing resources to guiding me through the process of learning basic computer programming. Thank you to Krish Mehta for collaborating with me on this project and taking the lead on the machine learning applications, all of your help was greatly appreciated. I'd like to acknowledge Lonny Lundsten and Larissa Lemon from MBARI's Video lab for helping with data management and providing resources and content for my presentation. The Bioinspiration lab (Joost Daniels, Paul Roberts, and Denis Klimov) for providing great feedback on my presentation. Special thanks to the MBARI internship coordinators (George Matsumoto, Megan Bassett, and Lyndsey Claassen) for not only running a great virtual internship but for also providing mentorship and support along the way.

Lastly, this project was generously supported by the National Science Foundation, NOAA, and through a gift from the Dean and Helen Witter Family Fund and the Rentschler Family Fund in memory of former MBARI board member Frank Roberts (1920-2019) and by the David and Lucile Packard Foundation.

References

Alldredge, A. L. (1984). The Quantitative Significance of Gelatinous Zooplankton as Pelagic Consumers. In M. J. R. Fasham (Ed.), Flows of Energy and Materials in Marine Ecosystems: Theory and Practice (pp. 407–433). Springer US. https://doi.org/10.1007/978-1-4757-0387-0_16

Boudreau, B. P., & Jorgensen, B. B. (2001). The Benthic Boundary Layer: Transport Processes and Biogeochemistry. Oxford University Press.

Choy, C. A., Haddock, S. H. D., & Robison, B. H. (2017). Deep pelagic food web structure as revealed by in situ feeding observations. Proceedings of the Royal Society B: Biological Sciences, 284(1868), 20172116. https://doi.org/10.1098/rspb.2017.2116

Gage, J. D., & Tyler, P. A. (1991). Deep-Sea Biology: A Natural History of Organisms at the Deep-Sea Floor. Cambridge University Press.

Gibson, R. N., & Barnes, M. (1997). Oceanography And Marine Biology: Volume 35. CRC Press.

Larson, R. J., Matsumoto, G. I., Madin, L. P., & Lewis, L. M. (1992). Deep-Sea Benthic and Benthopelagic Medusae: Recent Observations From Submersibles and a Remotely Operated Vehicle. Bulletin of Marine Science, 51(3), 277–286.

Matsumoto, G. I., Baxter, C., & Chen, E. H. (1997). Observations of the Deep-Sea Trachymedusa Benthocodon pedunculata. Invertebrate Biology, 116(1), 17–25. https://doi.org/10.2307/3226920

Matsumoto, G. I., Bentlage, B., Sherlock, R., Walz, K., & Robison, B. H. (2020). "Little Red Jellies" in Monterey Bay, California (Cnidaria: Hydrozoa: Trachymedusae: Rhopalonematidae). Frontiers in Marine Science, 0. https://doi.org/10.3389/fmars.2019.00798

R Core Team, 2013. R: A Language and Environment for Statistical Computing. R Foundation for Statistical Computing, Vienna, Austria, ISBN 3-900051-07-0. URL. http://www.R-project.org/.

RectLabel—Labeling images for bounding box object detection and segmentation. (n.d.). RectLabel. Retrieved August 12, 2021, from https://rectlabel.com

Redmon, J., Divvala, S., Girshick, R., & Farhadi, A. (2016). You Only Look Once: Unified, Real-Time Object Detection. ArXiv:1506.02640 [Cs]. http://arxiv.org/abs/1506.02640

Schlining, B. M., & Stout, N. J. (2006). MBARI's Video Annotation and Reference System. OCEANS 2006, 1–5. https://doi.org/10.1109/OCEANS.2006.306879

Smith, K. L. (1992). Benthic boundary layer communities and carbon cycling at abyssal depths in the central North Pacific. Limnology and Oceanography, 37(5), 1034–1056. https://doi.org/10.4319/lo.1992.37.5.1034

Smith, K. L., & Druffel, E. R. M. (1998). Long time-series monitoring of an abyssal site in the NE Pacific: An introduction. 15.

Smith, K. L., Huffard, C. L., McGill, P. R., Sherman, A. D., Connolly, T. P., Von Thun, S., & Kuhnz, L. A. (2020). Gelatinous zooplankton abundance and benthic boundary layer currents in the abyssal Northeast Pacific: A 3-yr time series study. Deep Sea Research Part II: Topical Studies in Oceanography, 173, 104654. https://doi.org/10.1016/j.dsr2.2019.104654

Station M Instrument Servicing Expedition 2018. (2018, October 18). MBARI. https://www.mbari.org/stationmservicing_expedition_2018/

Thomsen, L. (1999). Processes in the benthic boundary layer at continental margins and their implication for the benthic carbon cycle. Journal of Sea Research, 41(1), 73–86.

https://doi.org/10.1016/S1385-1101(98)00039-2

Vars-gridview. (2021). [Python]. Monterey Bay Aquarium Research Institute. https://github.com/mbari-org/vars-gridview (Original work published 2021)

Wishner, K. F. (1980). The biomass of the deep-sea benthopelagic plankton. Deep Sea Research Part A. Oceanographic Research Papers, 27(3), 203–216. https://doi.org/10.1016/0198-0149(80)90012-6